Role of material loss and mode volume of plasmonic nanocavities for strong plasmon-exciton interactions

Research Article | Vol. 24, No. 18 | 5 Sep 2016 | OPTICS EXPRESS 20373

Optics EXPRESS

Role of material loss and mode volume of plasmonic nanocavities for strong plasmon-exciton interactions

ZHONG-JIAN YANG,[1,2,4] TOMASZ J. ANTOSIEWICZ,[1,3,4] AND TIMUR SHEGAI[1,*]

[1]*Department of Physics, Chalmers University of Technology, 412 96, Göteborg, Sweden*
[2]*Hunan Key Laboratory of Super Microstructure and Ultrafast Process, School of Physics and Electronics, Central South University, Changsha, Hunan 410083, China*
[3]*Centre of New Technologies, University of Warsaw, Banacha 2c, 02-097 Warsaw, Poland*
[4]*These authors contributed equally.*
[*]*timurs@chalmers.se*

Abstract: We investigate the role of material loss and mode volume of plasmonic nanostructures on strong plasmon-exciton coupling. We find that the field enhancement, and therefore loss, is not important for the magnitude of the Rabi splitting as such, but instead it is determined by the mode volume. Nevertheless, for reaching true strong coupling condition, that is, coupling greater than any dissipation, it is important to compromise losses. We also show that using such popular geometries as a dimer of two spheres or bow-tie nanoantennas, does not allow compressing the mode volume much in comparison to a single nanoparticle case, except for very narrow gaps, but rather it allows for efficient extraction of the mode out of the metal thus making it more accessible for excitons to interact with. Even more efficient mode extraction is achieved when high refractive index dielectric is placed in the gap. Our findings may find practical use for quantum plasmonics applications.

OCIS codes: (250.5403) Plasmonics; (230.4555) Coupled resonators; (350.4238) Nanophotonics and photonic crystals.

References and links

1. J. McKeever, A. Boca, A. D. Boozer, J. R. Buck, and H. J. Kimble, "Experimental realization of a one-atom laser in the regime of strong coupling," Nature **425**, 268–271 (2003).
2. T. Volz, A. Reinhard, M. Winger, A. Badolato, K. J. Hennessy, E. L. Hu, and A. Imamoglu, "Ultrafast all-optical switching by single photons," Nature Photon. **6**, 605–609 (2012).
3. H.-K. Lo and H. F. Chau, "Unconditional security of quantum key distribution over arbitrarily long distances," Science **283**, 2050–2056 (1999).
4. G. Khitrova, M. Gibbs, M. Kira, S. W. Koch, and A. Scherer, "Vacuum Rabi splitting in semiconductors," Nature Phys. **2**, 81–90 (2006).
5. T. Aoki, B. Dayan, E. Wilcut, W. P. Bowen, A. S. Parkins, T. J. Kippenberg, K. J. Vahala, and H. J. Kimble, "Observation of strong coupling between one atom and a monolithic microresonator," Nature **443**, 671–674 (2006).
6. W. Barnes, A. Dereux, and T. Ebbesen, "Surface plasmon subwavelength optics," Nature **424**, 824–830 (2003).
7. P. Törmä and W. L. Barnes, "Strong coupling between surface plasmon polaritons and emitters: a review," Rep. Prog. Phys. **78**, 013901 (2015).
8. J. Bellessa, C. Bonnand, J. C. Plenet, and J. Mugnier, "Strong coupling between surface plasmons and excitons in an organic semiconductor," Phys. Rev. Lett. **93**, 036404 (2004).
9. J. Dintinger, S. Klein, F. Bustos, W. L. Barnes, and T. W. Ebbesen, "Strong coupling between surface plasmon-polaritons and organic molecules in subwavelength hole arrays," Phys. Rev. B **71**, 035424 (2005).
10. T. Schwartz, J. A. Hutchison, C. Genet, and T. W. Ebbesen, "Reversible switching of ultrastrong light-molecule coupling," Phys. Rev. Lett. **106**, 196405 (2011).
11. J. Bellessa, C. Symonds, K. Vynck, A. Lemaitre, A. Brioude, L. Beaur, J. C. Plenet, P. Viste, D. Felbacq, E. Cambril, and P. Valvin, "Giant rabi splitting between localized mixed plasmon-exciton states in a two-dimensional array of nanosize metallic disks in an organic semiconductor," Phys. Rev. B **80**, 033303 (2009).
12. S. R. K. Rodriguez and J. G. Rivas, "Surface lattice resonances strongly coupled to rhodamine 6g excitons: tuning the plasmon-exciton-polariton mass and composition," Opt. Express **21**, 27411–27421 (2013).
13. A. I. Väkeväinen, R. J. Moerland, H. T. Rekola, A.-P. Eskelinen, J.-P. Martikainen, D.-H. Kim, and P. Törmä, "Plasmonic surface lattice resonances at the strong coupling regime," Nano Lett. **14**, 1721–1727 (2014).

#269129 http://dx.doi.org/10.1364/OE.24.020373
Journal © 2016 Received 23 Jun 2016; revised 9 Aug 2016; accepted 12 Aug 2016; published 25 Aug 2016

Optics EXPRESS

14. G. Zengin, G. Johansson, P. Johansson, T. J. Antosiewicz, M. Käll, and T. Shegai, "Approaching the strong coupling limit in single plasmonic nanorods interacting with J-aggregates," Sci. Rep. **3**, 3074 (2013).
15. G. Zengin, M. Wersäll, S. Nilsson, T. J. Antosiewicz, M. Käll, and T. Shegai, "Realizing strong light-matter interactions between single-nanoparticle plasmons and molecular excitons at ambient conditions," Phys. Rev. Lett. **114**, 157401 (2015).
16. A. E. Schlather, N. Large, A. S. Urban, P. Nordlander, and N. J. Halas, "Near-field mediated plexitonic coupling and giant Rabi splitting in individual metallic dimers," Nano Lett. **13**, 3281–3286 (2013).
17. N. J. Halas, S. Lal, W.-S. Chang, S. Link, and P. Nordlander, "Plasmons in strongly coupled metallic nanostructures," Chem. Rev. **111**, 3913–3961 (2011).
18. E. Eizner, O. Avayu, R. Ditcovski, and T. Ellenbogen, "Aluminum nanoantenna complexes for strong coupling between excitons and localized surface plasmons," Nano Lett. **15**, 6215–6221 (2015).
19. K. Kneipp, Y. Wang, H. Kneipp, L. T. Perelman, I. Itzkan, R. R. Dasari, and M. S. Feld, "Single molecule detection using surface-enhanced raman scattering (sers)," Phys. Rev. Lett. **78**, 1667–1670 (1997).
20. S. Nie and S. R. Emory, "Probing single molecules and single nanoparticles by surface-enhanced Raman scattering," Science **275**, 1102–1106 (1997).
21. H. Xu, E. J. Bjerneld, M. Käll, and L. Börjesson, "Spectroscopy of single hemoglobin molecules by surface enhanced Raman scattering," Phys. Rev. Lett. **83**, 4357–4360 (1999).
22. T. J. Antosiewicz, S. P. Apell, and T. Shegai, "Plasmon–exciton interactions in a core-shell geometry: From enhanced absorption to strong coupling," ACS Photon. **1**, 454–463 (2014).
23. H. A. Atwater and A. Polman, "Plasmonics for improved photovoltaic devices," Nature Mater. **9**, 205–213 (2010).
24. T. Yoshie, A. Scherer, J. Hendrickson, G. Khitrova, H. M. Gibbs, G. Rupper, C. Ell, O. B. Shchekin, and D. G. Deppe, "Vacuum Rabi splitting with a single quantum dot in a photonic crystal nanocavity," Nature **432**, 200–203 (2004).
25. S. A. Maier, "Plasmonic field enhancement and SERS in the effective mode volume picture," Opt. Express **14**, 1957–1964 (2006).
26. X. Wu, S. K. Gray, and M. Pelton, "Quantum-dot-induced transparency in a nanoscale plasmonic resonator," Opt. Express **18**, 23633–23645 (2010).
27. S. Savasta, R. Saija, A. Ridolfo, O. Di Stefano, P. Denti, and F. Borghese, "Nanopolaritons: Vacuum rabi splitting with a single quantum dot in the center of a dimer nanoantenna," ACS Nano **4**, 6369–6376 (2010).
28. A. Manjavacas, F. J. G. d. Abajo, and P. Nordlander, "Quantum plexcitonics: Strongly interacting plasmons and excitons," Nano Lett. **11**, 2318–2323 (2011).
29. T. Hartsfield, W. S. Chang, S. C. Yang, T. Ma, J. Shi, L. Sun, G. Shvest, S. Link, and X. Li, "Single quantum dot controls a plasmonic cavity's scattering and anisotropy," Proc. Natl. Acad. Sci. U.S.A. **112**, 12288–12292 (2015).
30. K. Santhosh, O. Bitton, L. Chuntonov, and G. Haran, "Vacuum rabi splitting in a plasmonic cavity at the single quantum emitter limit," Nature Commun. **7**, 11823 (2016).
31. R. Chikkaraddy, B. de Nijs, F. Benz, S. J. Barrow, O. A. Scherman, E. Rosta, A. Demetriadou, P. Fox, O. Hess, and J. J. Baumberg, "Single-molecule strong coupling at room temperature in plasmonic nanocavities," Nature, https://www.repository.cam.ac.uk/handle/1810/255143 (2016).
32. A. F. Koenderink, "On the use of Purcell factors for plasmon antennas," Opt. Lett. **35**, 4208–4210 (2010).
33. C. Sauvan, J. P. Hugonin, I. S. Maksymov, and P. Lalanne, "Theory of the spontaneous optical emission of nanosize photonic and plasmon resonators," Phys. Rev. Lett. **110**, 237401 (2013).
34. P. T. Kristensen and S. Hughes, "Modes and mode volumes of leaky optical cavities and plasmonic nanoresonators," ACS Photon. **1**, 2–10 (2014).
35. C. Zhang, B.-Q. Chen, and Z.-Y. Li, "Optical origin of subnanometer resolution in tip-enhanced raman mapping," J. Phys. Chem. C **119**, 11858–11871 (2015).
36. W. W. Yu, L. Qu, W. Guo, and X. Peng, "Experimental determination of the extinction coefficient of cdte, cdse, and cds nanocrystals," Chem. Mater. **15**, 2854–2860 (2003).
37. D. Englund, I. Fushman, and J. Vuckovic, "General recipe for designing photonic crystal cavities," Opt. Express **13**, 5961–5975 (2005).
38. P. Johnson and R. Christy, "Optical constants of the noble metals," Phys. Rev. B **6**, 4370–4379 (1972).
39. P. Wróbel, T. Stefaniuk, M. Trzcinski, A. A. Wronkowska, A. Wronkowski, and T. Szoplik, "Ge wetting layer increases ohmic plasmon losses in Ag film due to segregation," ACS Appl. Mater. Interf. **7**, 8999–9005 (2015).
40. G. Zengin, T. Gschneidtner, R. Verre, L. Shao, T. J. Antosiewicz, M. Käll, and T. Shegai, "Evaluating conditions for strong coupling between nanoparticle plasmons and organic dyes using scattering and absorption spectroscopy," J. Phys. Chem. C, http://pubs.acs.org/doi/abs/10.1021/acs.jpcc.6b00219 (2016).

1. Introduction

Interaction of plasmons with excitons in molecules or quantum dots attracts considerable interest and research efforts in hopes of realizing high-end emerging applications like single-atom lasers [1], single-photon switches [2], and quantum cryptography [3] to name a few. Use of plasmonic nanostructures, rather than photonic crystals [4] and microring resonator cavities

Optics EXPRESS

[5], is dictated by the ability of the former to capture and guide light in deep subwavelength volumes [6]. Experimental and theoretical studies so far have demonstrated various degrees of interaction strengths between metal nanoparticles and excitons [7] in both large structures [8-13] as well single nanoparticles [14, 15] and dimer nanostructures [16]. These structures are in an overwhelming majority made either of silver or gold [17] – the workhorses of plasmonics due to low losses, though in principle in the UV aluminum is viable due to its optical properties [18].

Using Ag and Au means that the field enhancement near the surface of the metal nanoparticles easily exceeds one order of magnitude in the case of lone objects and for closely spaced dimers or rough surfaces can reach in excess of several hundreds. Interactions between plasmons and objects placed in these hot spots are thus greatly amplified leading to e.g. single molecule detection through Raman spectroscopy [19-21], enhanced absorption [22] and efficient solar harvesting [23].

It is usually accepted that in the case of plasmon-exciton nanostructures a large field enhancement is an important factor enabling strong coupling and Rabi splitting. This is true, however, simultaneously we stress that large field enhancement is *not* important for the values of Rabi splitting as such, as here we demonstrate virtually unchanged peak spitting for field enhancements spanning close to one decade. Although this seems surprising at first glance, in fact this just reflects that Rabi splitting alone is not an appropriate figure-of-merit for strong coupling. Rather the figure-of-merit should adequately consider losses. There are two alternative ways of doing this: (*i*) by taking a ratio between Rabi splitting and loss, $2g/\gamma_{\mathrm{pl}}$, and (*ii*) by considering cooperativity, $2g/\sqrt{\gamma_{\mathrm{pl}}\gamma_0}$, where g is the coupling strength and γ_{pl} and γ_0 are the plasmon and exciton dissipation rates, respectively. Importantly, both of these parameters scale with the field enhancement.

The coupling strength of plasmon-exciton hybrids is given by

$$g = \sqrt{N}\mu_{\mathrm{e}}|E_{\mathrm{vac}}|, \tag{1}$$

where N is the number of excitons coherently contributing to the coupling process, μ_{e} is the transition dipole moment of the interacting molecule, and

$$|E_{\mathrm{vac}}| = \sqrt{\hbar\omega/2\epsilon\epsilon_0 V} \tag{2}$$

is the vacuum field dependent on frequency ω and mode volume V [24]. Thus, the coupling strength is not explicitly dependent on the field enhancement, rather it is dependent on the mode volume. The field enhancement in turn is related to both V and Q of the nanocavity. As we show further the field enhancement, defined as $M = |E|/|E_0|$, is proportional to $Q/\sqrt{V}$ in agreement with Maier [25], which is exactly the figure-of-merit for strong coupling [4]. At the same time the vacuum Rabi splitting Ω is equal to $2g$ only in the limit of low loss as predicted by a coupled oscillator model [10,26,27]. In the case of non-negligible loss and zero detuning a simple coupled oscillator model predicts that Rabi splitting does depend on material parameters and in particular $\Omega = \sqrt{4g^2 - (\gamma_{\mathrm{pl}} - \gamma_0)^2}$ [10,27]. Thus our observation of nearly loss-independent splitting in case of plasmonic nanostructures is indeed quite puzzling and shows that in the case of high loss Rabi splitting might be confused with the Fano resonance in the weak coupling regime [26].

In this contribution we perform an in-depth study of various material-related and geometrical parameters on strong coupling between plasmons and excitons in the classical regime. This treatment is valid whenever the number of excitations in the system does not exceed the number of excitons [7]. For small structures considered here Ohmic losses dominate over radiative ones, which implies that material losses essentially determine Q of the plasmon resonance. We monitor the coupling strength as a function of the mode volume, that is, the distribution of electromagnetic energy density, $\rho = \epsilon|E|^2$, around the nanoantenna. In the first approximation the mode volume does not depend on the material loss, but instead it is determined by the arrangement of metal

Optics EXPRESS

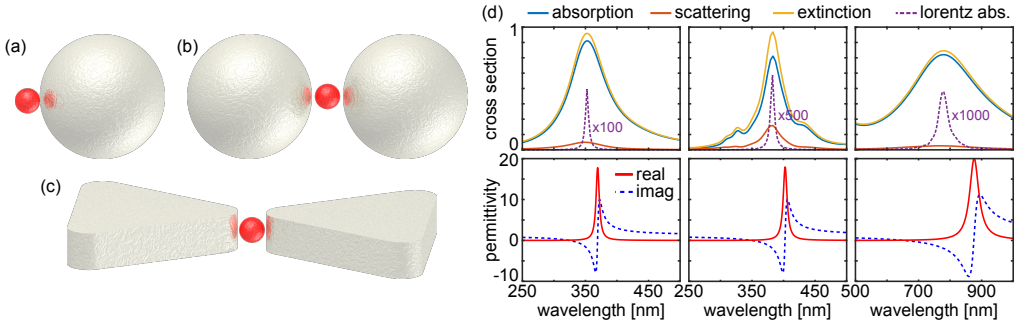

Fig. 1. Investigated metal-dye nanostructures. (a) Metal sphere $d_m = 30$ nm in diameter with a spherical dye particle $d_d = 5$ nm in size, separation of 2.5 nm. (b) Dimer of identical spheres as in (a) separated by 10 nm with a centrally placed dye particle. (c) Two thin nanoprisms with an edge of 70 nm, corner rounding 7 nm radius, and thickness of 10 nm. Prism separation is 10 nm and the dye particle is as previously. (d) Top row: cross sections of the metal nanostructure (solid lines) and absorption cross section of the Lorentz sphere (dashed line, multiplied by indicated factor for readability). Bottom row: real and imaginary parts of the Lorentz permittivity.

nanoparticles comprising the nanocavity. We study the effect of mode distribution and mode extraction on strong coupling. Finally, we show that upon sufficient compression of plasmonic modes, a single quantum dot may reach strong coupling with plasmon mode under realistic conditions. This latter observation although has been predicted theoretically [26-28], was reported in experiments only very recently [29-31] and should be further verified.

2. Model hybrid systems

In this study, we exploit three specific hybrid nanostructures as shown in Fig. 1, which we investigate using the finite-difference time-domain method (FDTD Solutions, Lumerical) and the T-Matrix method in one case as noted below. First, we consider a metal sphere of 30 nm diameter in whose vicinity we place a small dielectric sphere with dispersive permittivity mimicking that of a dye molecule. Maximum field enhancement near the metal nanosphere is about 10. Placing two spheres in a dimer arrangement [Fig. 1(b)] 10 nm apart pushes the field enhancement up to 30 at the center of the gap. Finally, we maximize the field enhancement by placing the dye nanoparticle between two triangular nanoprisms arranged in a bow tie fashion as in Fig. 1(c). In all these cases metal nanoparticle spectra are dominated by absorption, as illustrated by cross section plots shown in the top row of Fig. 1(d). Due to varying geometrical parameters, the resonance frequency of each nanostructure (sphere or both dimers) is different; hence, the parameters of the Lorentz permittivity of the dye change so that its absorption resonance coincides with that of the structure [note the dashed line in the top row of Fig. 1(d)]. However, to assure that conditions are equal despite varying resonance positions, the parameters of the Lorentz material are chosen such, that the transition dipole moment of the dye sphere is the same in all three cases and is equal to ~ 60 Debye. We intentionally use the transition dipole moment that is 2-4 times higher than realistic values of colloidal quantum dots to make the conclusions more instructive. Further, we consider more realistic transition dipole moment values. The parameters of the Lorentz spheres are summarized in Table 1 and the functions themselves are plotted in the bottom row of Fig. 1(d). The permittivity of the metal is described by a Drude function $\epsilon_{\text{metal}}(\omega) = 1 - \omega_p^2/(\omega^2 + i\gamma_p\omega)$, where ω is the (angular) frequency, $\hbar\omega_p = 6.25$ eV is the plasma energy, and γ_p is the collision frequency which varies from 0.2 to 2 eV.

Optics EXPRESS

Table 1. Lorentz permittivity $\epsilon_j(\omega) = 1 - f\omega_j^2/(\omega_j^2 - \omega^2 - 2i\gamma_j\omega)$ parameters used to model the optical properties of the dye: resonance frequency, line width, Lorentz permittivity, and transition dipole moment; λ_0 is the resonance wavelength of the nanostructure. These parameters give in all cases a transition dipole moment of $\mu_e = 60$ D.

	nanostructure		
paramter	sphere	sphere dimer	triangle dimer
λ_0 [nm]	353	383	780
ω_j [eV]	3.51	3.24	1.59
γ_j [meV]	30	30	30
f	0.3	0.33	0.8

3. Results

We begin by considering a simple case of a metal sphere placed adjacent to a Lorentz sphere. The extinction spectra [dominated by absorption, see Fig. 1(d)] are shown in Fig. 2 for five Drude damping values (with all other parameters constant). In all cases, interaction between the plasmon and exciton resonance results in a clear dip. The peak splitting, Ω, is constant (within calculation error) and equal to ~ 130 meV, as illustrated by the vertical dashed lines in the top row of Fig. 2. In order to appreciate the significance of a constant Ω, we analyze the optical properties of the metal resonator. Figure 2(d) displays the electric field enhancement generated by the metal sphere as measured at the position of the center of the Lorentz sphere (5 nm from the metal surface). Due to increasing damping, the enhancement decreases by a factor of more than 5 when increasing γ_p from 0.2 to 2 eV. However, this decrease of the field enhancement is not accompanied by a concomitant reduction of the peak splitting. Instead we observe a nearly constant splitting for all ranges of losses up to very high values of $\gamma_p = 2$ eV, which correspond to extremely bad plasmonic metals such as chromium. What does change with variation in material loss is the depth of the dip. We argue that despite observation of Rabi spitting in such lossy systems, one is hardly able of claiming strong coupling in this case, as the losses dominate over the coupling rate by more than one order of magnitude. Thus, it is important to realize that even if splitting is visible in the spectra, one cannot immediately conclude this is due to strong coupling [7].

Having observed that Ω does not vary, we calculate the mode volume of the metal sphere for each Drude damping parameter. The results are plotted with squares in Fig. 2(d) (right y-axis). There exist several approaches to calculating the mode volume of plasmonic nanostructures [32-34]. In particular we follow Koenderink [32] and define the mode volume as

$$V = \int \eta(\mathbf{r}) dV, \tag{3}$$

where

$$\eta(\mathbf{r}) = \rho(\mathbf{r})/\rho_{max} \tag{4}$$

describes the spatial extent of the mode with $\rho(\mathbf{r}) = \epsilon(\mathbf{r})|E(\mathbf{r})|^2$ being the energy density at the position $\mathbf{r}$, and $\rho_{max} = \max(\epsilon(\mathbf{r})|E(\mathbf{r})|^2)$. Note that integration goes both inside and outside metal. The results show that while not exactly constant, V varies much less than the field enhancement, with the variations caused by inaccuracies in our calculations. Since E_{vac} is proportional to $1/\sqrt{V}$, any small fluctuations become negligible. Using an average value $V = 1.3 \times 10^4$ nm^3 and the value of the transition dipole moment – 60 D, we obtain $g = 60$ meV, which gives $\Omega = 120$ meV, in agreement with what is measured in Fig. 2(a). Thus, spatial energy density V does not follow the material loss, which in turn results in constant splitting – Ω.

Optics EXPRESS

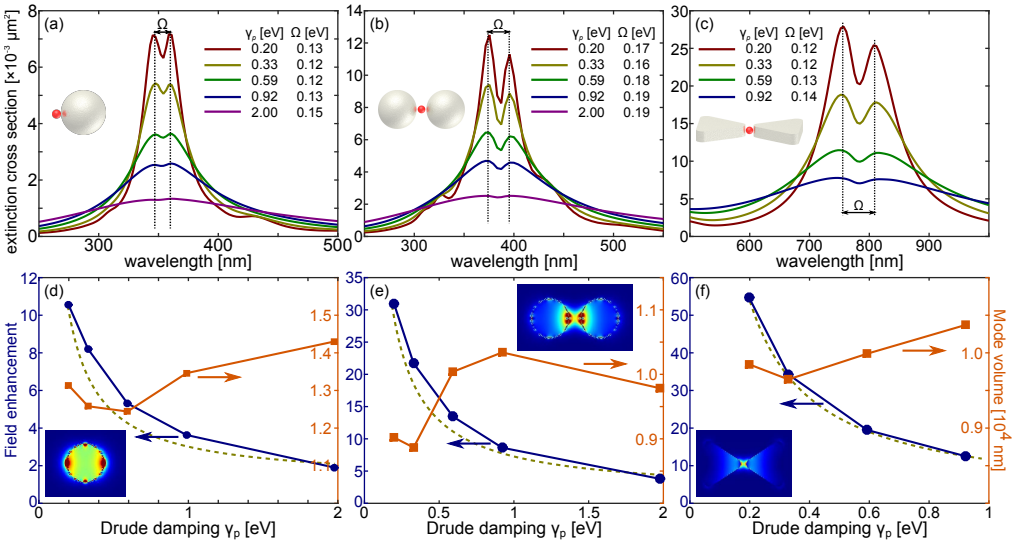

Fig. 2. (a-c) Extinction cross sections of a coupled metal sphere – dye nanoparticle structure. The damping of the metal increases by one order of magnitude and the peak splitting Ω (see the vertical dotted lines and the table) remains practically constant, only its visibility decreases up to a point when it almost disappears for the highest losses $\gamma_p = 2$ eV. (d-f) Field enhancement at the center of the Lorentz nanosphere (left y-axis, circles) and mode volume of the Drude metal sphere (right y-axis, squares) as function of the loss parameter γ_p of the metal sphere. Note the considerable decrease of the field enhancement accompanied by an almost constant mode volume. Extinction cross sections of dimers composed of (a) two spheres and (c) two triangles coupled to a dye nanoparticle. (b,d) Field enhancements (left y-axis) and mode volumes (right y-axis) of the sphere dimer and triangle dimer structures, respectively. The field enhancement values for the dimers are considerably larger than for the single sphere, yet the peak splitting, when normalized to the resonance energy of the plasmonic structure, is only slightly larger for the dimers. The mode volumes are, on the other hand, slightly smaller for the dimers than the single sphere, in agreement with the peak splitting dependence. Note, that while the field enhancement is strongly dependent on the damping, the mode volume and the peak splitting are not.

To verify if such a picture holds in other types of plasmonic resonators, we now turn to structures with much larger field enhancements – nanoparticle dimers. The optical spectra of sphere- and triangle-dimers coupled to the Lorentz spheres are shown in Fig. 2(b,e) and Fig. 2(c,f) respectively. Measured splitting is 160-190 meV and 120-140 meV for dimers made of spheres and triangles, respectively. Comparing these values to the field enhancements for various loss parameters calculated at the positions of the Lorentz spheres [Fig. 2(e,f)] we note again the lack of any relationship. Only when we analyze the mode volume, which in both cases is lower than for the sphere, though not by a lot, we see again the basis for stable splitting. Estimating the coupling rates g from the calculated mode volumes $V = 1.0 \times 10^4$ nm^3 and taking into account red shift in the plasmon resonance frequency for the dimer structures we get ~66 meV and 47 meV, respectively. These values compare rather well with the splitting that is read off the cross section plots, however, we observe that the equation for the coupling rate $g = \mu_e |E_{vac}|$ does underestimate the splitting in case of dimer structures by about 20%. We note that a small reduction in the mode volume (from 1.3×10^4 nm^3 to 1.0×10^4 nm^3) cannot account for larger splitting in case of dimers even after taking the plasmon resonance shifts into account. This extra splitting arises from (*i*) better mode overlap between excitons and plasmons in case of dimer

Optics EXPRESS

structures, as the maximum energy density $\rho_{\max}$ is efficiently pulled out of the metal due to nanoparticle interaction and (*ii*) additional mode concentration in the gap region due to presence of high refractive index dielectric [35]. Indeed, the energy density plots show that the maximal energy density is located inside metal for the single sphere [inset Fig. 2(d)], while it is mostly concentrated in the gap region for both dimer nanostructures [insets Fig. 2(e,f)]. Based on these observations, in the remaining part of the manuscript, we focus on properties of the mode in terms of its localization and distribution. This knowledge is essential for optimizing plasmon exciton interactions.

We start by studying the effect of mode overlap between excitons and plasmons (see Fig. 3, here we used the T-Matrix method). The spatial extent of the mode, $\eta(\mathbf{r}) = \rho(\mathbf{r})/\rho_{\max} \leq 1$, not only determines V but also allows to calculate the field enhancement and the Rabi splitting at arbitrary position $\mathbf{r}$ near the nanostructure. Both $M(\mathbf{r})$ and $\Omega(\mathbf{r})$ scale as $\sim \sqrt{\eta(\mathbf{r})}$, which describes the distribution of local density of states around the nanoantenna. By displacing the Lorentz sphere up to 16 nm away from the center of the dimer, different local density of states is probed [Fig. 3(a)]. In agreement with the above, the splitting becomes smaller and the dip shallower. This can be compared to

$$\Omega(\mathbf{r}) = 2\sqrt{\eta(\mathbf{r})}\mu_e|E_{\text{vac}}|. \tag{5}$$

In Fig. 3(b) we show that full calculation and a simple extraction based on the mode volume agree qualitatively, but quantitatively there is a 1.6× mismatch. This apparent mismatch arises from additional mode compression, due to presence of high refractive index dielectric in the gap region [35]. We study this effect in Fig. 4. For a test case of a silver bow-tie we calculate its mode volume taking into account also the background permittivity of the quantum dot, although we vary ϵ_∞ beyond what is typically observed at optical frequencies for quasi-dispersionless dielectrics. This way the resonator, whose V is required for a realistic calculation, consists of the bow-tie with the dielectric particle in the gap and this entity couples to the transition dipole moment in the quantum dot. For typical CdSe quantum dots ($\epsilon_\infty \approx 6$) the decrease is significant as shown in Fig. 4. In our case it exactly matches the 1.6× factor used in Fig. 3 by which the calculated dependence is multiplied to match the observed peak splitting.

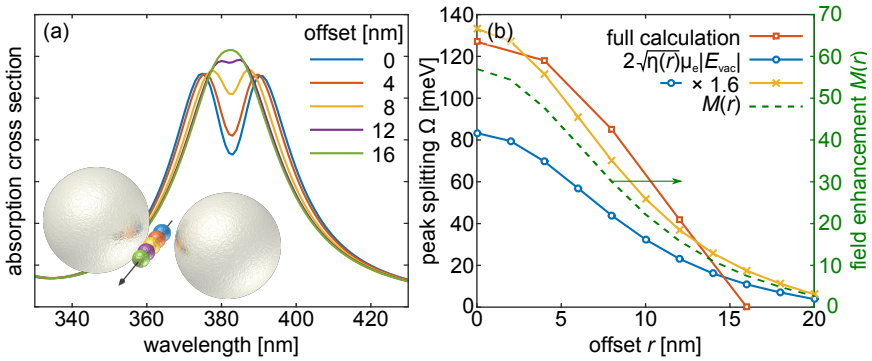

Fig. 3. (a) Absorption cross sections for sphere dimers with the Lorentz nanoparticle moving out of the hot spot as indicated in the inset. The electric field is polarized along the axis joining the two metal spheres. As the exciton leaves the hot spot and experiences a deceasing field enhancement the peak splitting decreases (mainly due to smaller overlap between the molecules and the mode) and the dip becomes shallower (mainly due to a weaker field) in line with $\Omega(\mathbf{r}) = 2\sqrt{\eta(\mathbf{r})}\mu_e|E_{\text{vac}}|$. (b) Comparison of measured (squares) and calculated (circles) splitting. The calculated splitting is multiplied by ca. 1.6 to match the measured values (see Fig. 5).

Optics EXPRESS

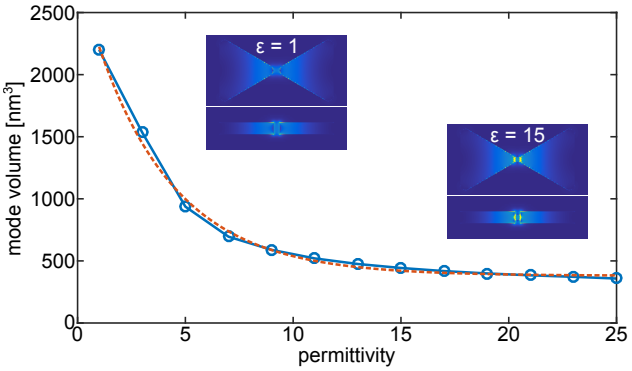

Fig. 4. Compression of the mode volume of a silver bow-tie dimer loaded with a 4 nm dielectric sphere in the gap as a function of the sphere's permittivity. Increase of ϵ from 1 to 25 deceases the mode volume to ca. 0.2 of the initial value. Although 25 is unrealistic at optical frequencies, $\epsilon_\infty = 6$ is typical for quantum dots and this decreases V about 2.5 times, which increases the coupling strength 1.6-fold. This is consistent with the multiplicative factor used in Fig. 3.

We now turn to the role of the mode volume itself. By appropriately designing the nanostructure the mode volume can be made very small, however, there are limits to what can be achieved [25, 32-34]. For single metal nanoparticles in the 50 nm size range V is smaller than the physical volume; however, as the diameter decreases the mode volume approaches the physical one [32]. In Fig. 2(a) we see that the mode volume is well approximated by the geometrical volume of the spherical nanoparticle $4\pi R^3/3$ for $R = 15$ nm, which is $V_{\text{geom}} = 1.4 \times 10^4$ nm^3. Thus, an appreciable increase of the coupling rate can be achieved by shrinking the particle diameter. An alternative way of compressing the mode is to utilize dimers to localize the electric field in the gap. In Fig. 5(a) we show field enhancement and mode volume for the bowtie geometry calculated as a function of interparticle gap within the range of 1-10 nm. We show that for 1 nm gap the mode can be compressed as much as $V = 300$ nm^3, which is about 10^2 times more compact than for an isolated particle and about 10^6 than the diffraction limit λ^3.

Strong compression of the mode volume, among other things, implies that a single quantum emitter with a realistic value of transition dipole moment may reach the strong coupling regime. To demonstrate this, in Fig. 5(c) we show that a 7 nm gap bowtie can produce splitting with an individual quantum emitter placed inside the gap and for realistic parameters ($\mu_e \approx 13$ D) of colloidal CdSe quantum dots and exciton width corresponding to low temperature studies [26,36]. Thus a single nanoantenna – single quantum emitter geometry is indeed feasible and promising for quantum optics using plasmonic nanocavities, but at the same time that no unrealistically low losses on the metal side is necessary. We note though that as the gap is reduced, the resonance shifts to the red rather considerably (note that mode volumes were always calculated at the resonance wavelength).

Finally, we would like to mention that analysis of strong coupling in terms of the Q and V allows to draw a connection between them and the field enhancement. In particular from Fig. 5(a) we learn that the field enhancement depends on the mode volume in accordance with $M \sim 1/\sqrt{V}$ [dashed line in Fig. 5(a)], provided Q is constant. From Fig. 2, on the other hand, we observe that $M \sim Q$ (see dashed lines in panels d-f), provided V is constant. By merging these two observations together we obtain $M \sim Q/\sqrt{V}$ in agreement with previous studies [25, 37]. This is precisely the figure-of-merit for strong coupling, which implies that one should maximize M but at the same time this is not crucial for Ω.

Optics EXPRESS

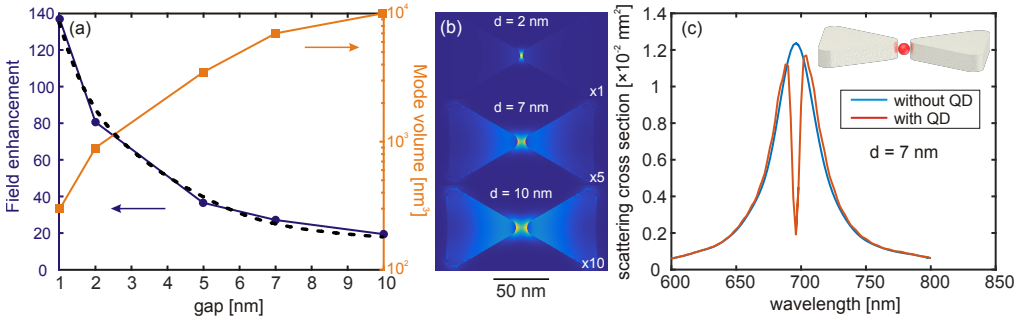

Fig. 5. (a) Dashed line shows $M \sim 1/\sqrt{V}$. Blue circles is an actual calculation of the field enhancement. Orange squares is calculated V. For all points loss is 0.59 eV. (b) Energy density distribution at loss equal 0.59 eV. (c) Scattering cross-section of a silver bow-tie nanoantenna loaded with (red) and without (blue) a CdSe QD having $\mu = 13$ D ($\epsilon_\infty = 6$, $f = 0.1$, line position 1.77 eV, width 5 meV).

4. Conclusions

In this work we have made a surprising observation that the mode volume and thus the splitting does not depend on material loss. In particular, the three nanostructures we have investigated clearly demonstrate that to observe plasmon-exciton peak splitting it is not critical to have low loss materials. The smallest loss we considered, 200 meV, is approximately one order of magnitude larger than in the lowest accepted Drude fits of experimental data of Johnson and Christy for silver [38], however, other experiments report larger losses and hence a greater imaginary part [39]. Yet for all $\gamma_p \in (0.2, 2)$ eV we observe a constant peak splitting. We argued that judging on whether all the spectra shown in Fig. 2 can be attributed to strong coupling based solely on observation of splitting may be misleading. Instead, more thoroughly one should observe anti-crossing in absorption of a strongly coupled system [40]. This is hard to achieve in experiments, therefore one should optimize strong coupling in terms of e.g. cooperativity.

We have also analyzed the mode volume and its overlap with excitons. Our findings indicate that while dimer structures are not able to compress the mode much in comparison to individual nanoparticles (except for very narrow gaps), instead extract the mode out of the metal and thus make it accessible for interaction with excitons. Finally, we note that plasmonic modes can be compressed in sharp gaps and placing high dielectrics in the gap region, though to a limit of about ~100 nm^3, which opens up possibilities for strong coupling with individual quantum emitters and thus possible quantum optics applications.

Funding

We acknowledge financial support from Knut and Alice Wallenberg Foundation and the Swedish Foundation for Strategic Research. TJA acknowledges support from the Polish Ministry of Science and Higher Education via the Iuventus Plus project IP2014 000473 and the Foundation for Polish Science for support via the project HOMING PLUS/2013-7/1. TS acknowledges support from Swedish Research Council (VR, grant number: 2012-04014).